Catalysis Science & Technology

PAPER

View Article Online
View Journal | View Issue

Cite this: *Catal. Sci. Technol.*, 2016, **6**, 4849

Hierarchically structured ZSM-5 obtained by optimized mesotemplate-free method as active catalyst for methanol to DME conversion

M. Rutkowska,*[a] D. Macina,[a] Z. Piwowarska,[a] M. Gajewska,[b] U. Díaz[c] and L. Chmielarz[a]

Received 7th January 2016,
Accepted 23rd February 2016

DOI: 10.1039/c6cy00040a

www.rsc.org/catalysis

In the presented studies, a new method for the synthesis of hierarchical porous materials with ZSM-5 zeolite properties was applied. The proposed method is based on the acidification of the zeolite seeds slurry using HCl solution, followed by hydrothermal treatment, enabling the aggregation of zeolite nanoseeds with the formation of the interparticle mesoporous structure. The influence of the duration of zeolite parent mixture aging before and after acidification on the resulting properties of the samples was investigated. The physicochemical properties of the obtained micro-mesoporous samples were analyzed using techniques such as N_2-sorption measurements, X-ray diffraction, TG analysis, NH_3-TPD and electron microscopy. In the second part of the studies, the influence of the modified zeolite sample parameters (such as porosity, acidity and crystallinity) on their catalytic activity for dimethyl ether (DME) synthesis from methanol was studied. DME is considered as a future clean alternative to diesel fuel and the development of methods for its synthesis is currently of high scientific interest. It was shown that modification of the porous structure and acidity of the zeolitic samples strongly influences their catalytic activity, selectivity and stability for the DME synthesis process. The micro-mesoporous samples, despite their significantly lower acidity, exhibited high catalytic activity (similar to conventional ZSM-5 zeolite) and enhanced selectivity towards DME, as well as higher stability in a long term catalytic test (higher resistance to the formation of coke deposits) in comparison to standard MFI-type zeolites.

1. Introduction

Hierarchical zeolites, containing both micro- and mesopores, are a new and rapidly developing group of materials. Among this group of materials, specific interest has been devoted to the generation of mesopores in the ZSM-5 zeolite structure (MFI topology), which is known to be very active in many catalytic reactions. It is expected that the presence of mesopores should minimalize internal diffusion limitations and enhance the overall effectiveness of the catalytic processes. During recent years, different approaches have been applied to synthesize micro-mesoporous ZSM-5 zeolite. One of the most widely studied methods was based on destructive post-synthesis treatments – desilication and dealumination (controlled removal of framework Si and Al in basic and acidic medium, respectively).[1–4] Moreover, many constructive methods were proposed in the literature, such as carbon, polymer or soft (surfactant) templating[5–7] or methods based on the synthesis and controlled alignment of ZSM-5 sheets. The group of Prof. Ryoo[8,9] synthesized MFI nanosheets of 2 nm thickness using an organic surfactant functionalized with a diquaternary ammonium group in the head (*e.g.* $C_{22}H_{45}$–$N^+(CH_3)_2$–C_6H_{12}–$N^+(CH_3)_2$–C_6H_{13}) as a structure directing agent for the intercalation of silica pillars into the zeolite interlayer space. The diameter of mesopores generated in the interlayer space could be tailored by the modification of the surfactant structure, especially the hydrocarbon tail length. Zhang *et al.*[10] reported the successful synthesis of self-pillared nanosheets of MFI (using a one-step hydrothermal synthesis method) with a house-of-cards structure and mesopores in the range of 2–7 nm.

From the economic and environmental points of view, the most promising routes seem to be the one-pot synthesis methods, resulting in hierarchical materials being obtained in a one-step procedure without the use of expensive surfactants for mesopore formation. One of the possible options is a mesotemplate-free method, based on the controlled aggregation of zeolite nanoseeds[11] with the formation of the interparticle mesoporous structure. This approach was previously

[a] *Jagiellonian University, Faculty of Chemistry, Ingardena 3, 30-060 Kraków, Poland. E-mail: rutkowsm@chemia.uj.edu.pl; Fax: +48 126340515; Tel: +48 126632096*
[b] *AGH University of Science and Technology, Academic Centre for Materials and Nanotechnology, Mickiewicza 30, 30-059 Kraków, Poland*
[c] *Instituto de Tecnología Química, UPV-CSIC, Universidad Politécnica de Valencia, Avenida de los Naranjos, s/n, 46022 Valencia, Spain*

applied by Rutkowska *et al.*[12,13] and Van Oers *et al.*[14,15] and concerned the synthesis of micro-mesoporous materials with Beta zeolite properties. In this work, a new mesotemplate-free method for micro-mesoporous ZSM-5 synthesis is presented, and the catalytic efficiency of the obtained materials in the synthesis of dimethyl ether (DME) from methanol is investigated.

Dimethyl ether, due to its unique properties such as its high cetane number, lack of C–C bonds, a vapor pressure similar to LPG and its atoxicity, has gained great attention of scientists as a promising clean alternative fuel.[16,17] DME can be used as an LPG (similar physico-chemical properties allow the use of existing infrastructures for transportation and storage) and a diesel fuel substitute (lower soot emission in comparison to conventional fuels). Moreover, DME can be used as a petroleum gas for heating and home cooking (burning with a visible blue flame) or as a substrate of many chemical reactions (low-poisoning alternative of methanol), *e.g.* being converted to light olefins or aromatics. DME can be synthesized directly from syngas (produced from natural gas, coal or biomass) using a bifunctional catalyst ($2CO + 4H_2 \rightarrow CH_3OCH_3 + H_2O$) or by an indirect method from methanol using an acid catalyst ($2CH_3OH \rightarrow CH_3OCH_3 + H_2O$). A growing awareness of climate change, air pollution and continuously increasing energy consumption makes DME an attractive green alternative to cut down greenhouse gas emission and to recycle the stored resources of CO_2 (in the case of the direct synthesis method).

ZSM-5 zeolite was found to be an active and stable catalyst for the MTD process (methanol to DME), especially in the presence of water. The high catalytic activity of this zeolite results from the presence of Brønsted acid sites, which are responsible for adsorption and conversion of methanol.[18] The strength of the acid sites is very important in the MTD process because too strong acid sites may result in the deposition of carbonaceous species, which hinders the access of methanol to the active centers and blocks the pores of the zeolite. This undesired effect can be overcome by modification of the porous structure and the acidity of ZSM-5 zeolite.[19,20]

To the best of our knowledge, only a few papers regarding the catalytic performance of micro-mesoporous systems with ZSM-5 zeolite properties in the synthesis of DME were published. In our previous studies[21] we examined micro-mesoporous ZSM-5 obtained by desilication of the parent zeolite with 0.1 M NaOH solution for 1, 2 and 4 h. The desilicated samples exhibited higher catalytic activity and stability in DME synthesis in comparison to the conventional zeolite. Wei *et al.*[22] investigated the catalytic activity of desilicated ZSM-5 (using 0.2 M NaOH) with different Si/Al ratios, and reported an improvement in the selectivity to DME. This effect was related to the enhanced diffusion capability in the micro-mesoporous samples. Yang *et al.*[23] examined hierarchical ZSM-5 synthesized using two kinds of templates simultaneously for micro- and mesopore generation (tetrapropylammonium hydroxide and dimethyldiallyl ammonium chloride acrylamide copolymer, respectively). Mesoporous ZSM-5 obtained by this method exhibited better stability (higher resistance to coke formation) in comparison to conventional ZSM-5. Another interesting group of micro-mesoporous catalysts for the MTD reaction are ZSM-5/MCM-41 composites (showing better selectivity towards DME in comparison to conventional ZSM-5), prepared by hydrothermal techniques using nanosized ZSM-5 particles.[24–26]

Taking into account the benefits resulting from the presence of mesopores in the structure of catalysts with MFI topology in the MTD reaction, a new one-step method for hierarchical ZSM-5 synthesis was proposed. In this work, the influence of the hydrothermal synthesis parameters on the physicochemical properties of the micro-mesoporous samples and their activity, selectivity and stability for dimethyl ether synthesis from methanol was studied.

2. Experimental methods

2.1. Catalyst preparation

The samples with ZSM-5 zeolite properties were prepared according to the modified procedure described in 'Verified Synthesis of Zeolitic Materials' for high alumina ZSM-5.[27] Tetrapropylammonium hydroxide (TPAOH, 20% in H_2O, Sigma-Aldrich) was used as a structure-directing agent, while tetraethyl orthosilicate (TEOS, 98%, Sigma-Aldrich) and $NaAlO_2$ (Sigma-Aldrich) acted as silica and aluminium sources, respectively.

In the first stage, seeding gel was prepared by mixing TPAOH with an aqueous solution of NaOH, followed by dropwise addition of TEOS. The resulting slurry was mixed for 1 h and then hydrothermally aged in an autoclave at 100 °C for 16 h.

In the second step, the synthesis gel was prepared by mixing 5 g of the obtained earlier seeding gel with an aqueous solution of NaOH and $NaAlO_2$, followed by dropwise addition of TEOS. The resulting solution with the molar composition of $SiO_2 : 0.03Al_2O_3 : 0.11Na_2O : 30H_2O$ (exclusive of the seeding gel) was hydrothermally treated at 150 °C for 7 days (in the case of conventional ZSM-5) and for 24, 48 or 72 h (in the cases of the hierarchical porous samples). After an appropriate time (24, 48 or 72 h) of hydrothermal aging, the protozeolitic seeds were acidified in a proportion of 5 mL of concentrated HCl per 10 mL of the nanoseed slurry. Subsequently, the acidified slurries were hydrothermally treated for a second time at 150 °C for 144, 120 or 96 h, yielding micro-mesoporous ZSM-5 zeolite. After the aging periods, all the autoclaves were quenched and the samples were filtered, washed with distilled water, dried in ambient conditions and calcined at 600 °C for 6 h.

The as-synthesized samples were denoted as follows: as-ZSM-5 (aging duration before acidification – 24, 48 or 72 h/aging duration after acidification – 144, 120 or 96 h). The aging duration after acidification was adjusted to keep the total aging duration at 7 days (as in the case of conventional ZSM-5). Among this group of the samples, an optimum aging duration before acidification of 48 h was chosen. For this sample, an

influence of the aging duration after acidification on its physico-chemical properties was determined. This series of samples was denoted as as-ZSM-5 (48/aging duration after acidification – 24 or 48). All the sample codes and the parameters of their synthesis are presented in Table 1.

The as-synthesized samples (in Na-forms, in case of the hierarchical samples being partially H-exchanged during acidification) were triply exchanged with a 0.5 M solution of NH_4NO_3 (Sigma-Aldrich) at 80 °C for 1 h, filtered, washed with distilled H_2O and dried in ambient conditions. Finally, the samples were calcined at 600 °C for 6 h to convert them to their H-forms.

2.2. Catalyst characterization

The textural properties of the samples were determined by N_2 sorption at −196 °C using a 3Flex v1.00 (Micromeritics) automated gas adsorption system. Prior to the analysis, the samples were degassed under vacuum at 350 °C for 24 h. The specific surface area (S_{BET}) of the samples was determined using BET (Braunauer–Emmett–Teller) model according to the recommendations of Rouquerol *et al.*[28] The micropore volume and specific surface area of the micropores were calculated using the Harkins and Jura model (*t*-plot analysis, thickness range 0.55–0.85 nm). The mesopore volume was calculated from the desorption branch using the BJH model (Kruk–Jaroniec–Sayari empirical procedure) in the range of 17–300 Å.

The X-ray diffraction (XRD) patterns of the samples were recorded using a Bruker D2 Phaser diffractometer. The measurements were performed in the 2 theta range of 5–50° with steps of 0.02°.

Thermogravimetric measurements were performed using a TGA/SDTA851e Mettler Toledo instrument connected with a quadrupole mass spectrometer ThermoStar (Balzers). The samples were heated in a flow of synthetic air (80 mL min^{-1}) with the ramping of 10 °C min^{-1}, in the temperature range of 70–1000 °C.

The Si/Al ratio in the samples was analyzed by means of atomic absorption spectroscopy (Spectra AA 10 Plus, Varian).

The surface acidity (concentration and strength of acid sites) of the samples was studied by temperature-programmed desorption of ammonia (NH_3-TPD). The measurements were performed in a flow microreactor system equipped with a QMS detector (UMS TD Prevac). Prior to ammonia sorption, a sample was outgassed in a flow of pure helium at 600 °C for 30 min. Subsequently, the microreactor was cooled to 70 °C and the sample was saturated in flow of a gas mixture containing 1 vol% of NH_3 diluted in helium for about 120 min. Then, the catalyst was purged in a flow of helium until a constant base line level was attained. Desorption was carried out with a linear heating rate (10 °C min^{-1}) in a flow of He (20 ml min^{-1}). Calibration of the QMS with commercial mixtures allowed recalculation of the detector signal into the rate of NH_3 evolution.

Transmission electron microscopy (TEM) investigations were carried out using a FEI Tecnai TF20 X-TWIN (FEG) microscope, equipped with an EDAX energy dispersive X-ray (EDX) detector, at an accelerating voltage of 200 kV.

The chemical nature of the coke deposit formed during the catalytic reaction was studied by UV-vis-DR spectroscopy. Measurements were performed using an Evolution 600 (Thermo) spectrophotometer in the range of 200–900 nm with a resolution of 2 nm.

2.3. Catalytic tests

Catalytic experiments for the process of DME synthesis from methanol were performed in a fixed-bed quartz microreactor system under atmospheric pressure in the temperature range from 100 to 325 °C in intervals of 25 °C. For each test, 0.1 g of catalyst with a particle size between 0.160 and 0.315 mm was outgassed in a flow of pure helium at 300 °C for 1 h. After cooling down to 100 °C, a gas mixture containing 4 vol% of methanol diluted in pure helium (total flow rate of 20 ml min^{-1}) was supplied into the microreactor using an isothermal saturator (0 °C). To avoid any product condensation during the reaction run, the gas lines were heated to 120 °C using heating tapes. The outlet gases were analyzed using a gas chromatograph (SRI 8610C) equipped with a Haysep D column, methanizer and FID detector. Additionally, catalytic stability tests (50 h of continuous work) and hydrothermal stability tests (in the presence of water vapor) at 250 °C were carried out for the H-ZSM-5 and H-ZSM-5 (48/120) samples.

3. Results and discussion

3.1. Synthesis and characterization

Textural parameters of the as-synthesized samples, determined by nitrogen sorption measurements, are presented in Table 2. The BET surface area of the hierarchical samples is lower in comparison to the reference conventional as-ZSM-5. The value of S_{BET} increased upon increasing of the aging

Table 1 Sample codes and synthesis conditions

Sample code	Aging duration before acidification/h	Aging duration after acidification/h	Total aging duration/days
as-ZSM-5	—	—	7
as-ZSM-5 (24/144)	24	144	7
as-ZSM-5 (48/120)	48	120	7
as-ZSM-5 (72/96)	72	96	7
as-ZSM-5 (48/24)	48	24	3
as-ZSM-5 (48/72)	48	72	5

Table 2 Textural properties of the as-synthesized samples determined from the N_2-sorption measurements and Si/Al ratios of the samples

Sample code	S_{BET}/m^2 g^{-1}	S_{MIC}/m^2 g^{-1}	V_{MIC}/cm^3 g^{-1}	V_{MES}/cm^3 g^{-1}	Si/Al
as-ZSM-5	379	371	0.145	0.024	12
as-ZSM-5 (24/144)	30	20	0.009	0.019	18
as-ZSM-5 (48/120)	300	277	0.119	0.105	22
as-ZSM-5 (72/96)	301	279	0.118	0.077	19
as-ZSM-5 (48/24)	157	114	0.049	0.069	34
as-ZSM-5 (48/72)	195	165	0.071	0.092	35
H-ZSM-5/stab	71	52	0.024	0.031	—
H-ZSM-5 (48/120)/stab	228	196	0.083	0.068	—
H-ZSM-5/H_2O	394	376	0.159	0.061	—
H-ZSM-5 (48/120)/H_2O	267	239	0.101	0.068	—

duration before acidification to reach 300 m^2 g^{-1} after 48 h (it seems that further prolongation of the aging duration before acidification does not significantly influence the value of S_{BET}). These changes were accompanied by a decrease in the micropore volume and the area of the acidified samples in comparison to the conventional zeolite. In the case of these parameters, we also observed an increase upon increasing the aging duration before acidification to obtain a constant level after 48 h. However, a decrease in the microporosity volume observed after acidification occurred in favor of a significant increase (four times in the case of as-ZSM-5 (48)) in the mesopore volume of the hierarchical samples. An increase in the volume of mesopores proves the successful generation of mesopores in the acidified as-ZSM-5 (48/120) and as-ZSM-5 (72/96) samples.

Based on the textural parameters obtained by N_2-sorption measurements, it could be concluded that the duration of nucleation of zeolitic seeds before acidification is a very important parameter affecting the final properties of the hierarchical samples. In case of the ZSM-5 zeolite, conducting the hydrothermal ageing process for 24 h was not enough to generate the microporous structure, however, extending the aging duration to 48 h seems to be sufficient to crystalize MFI protozeolitic seeds (giving about 80% of the as-ZSM-5 micropore volume) and prolongation of this time does not significantly influence the microporosity development of the samples. On the other hand, the acidification of the synthesis gel resulted in the generation of significant mesoporosity in the case of both the as-ZSM-5 (48/120) and as-ZSM-5 (72/96) samples, greater than in the cases of as-ZSM-5 and as-ZSM-5 (24/144). Taking into account economic issues (shorter aging duration at 150 °C) the 48 h aging procedure was chosen as the optimal procedure, and in the next step of our research, an influence of the aging duration time after acidification on the textural parameters of the samples was verified.

The shortening of the aging duration after acidification resulted in a decrease of all textural parameters, both related to the micro- and mesoporosity of the samples. Thus, it could be concluded that the crystallization time after acidification also plays a very important role in the formation of the hierarchical porous structure.

The nitrogen adsorption–desorption isotherms recorded for the as-synthesized samples are shown in Fig. 1. An isotherm of type I(a) (according to IUPAC classification[29]), characteristic of microporous structure, was obtained for the as-ZSM-5 sample (Fig. 1a). While in case of the acidified samples, adsorption–desorption isotherms of IV(a) type with hysteresis loops characteristic of mesoporous materials were obtained.

The very low value of adsorbed N_2 volume in case of the as-ZSM-5 (24/144) sample, connected with the lack of an uptake step at very low p/p_0 values proved that 24 h of hydrothermal aging before acidification was not enough to effectively create the microporous ZSM-5 structure. In the cases of as-ZSM-5 (48/120) and as-ZSM-5(72/96), the shape of the hysteresis loop can be classified as H5 type (associated with pore structures containing both open and partially blocked mesopores). A very interesting change in the shape of the hysteresis loop was observed after modification of the aging duration after acidification (Fig. 1b).

Together with the shortening of the aging time after acidification, the loop of type H5 changed to a loop of H4 type (often obtained in the case of mesoporous zeolites). Thus, it could be concluded that the duration of hydrothermal treatment after acidification strongly influences the shape of the created mesopores.

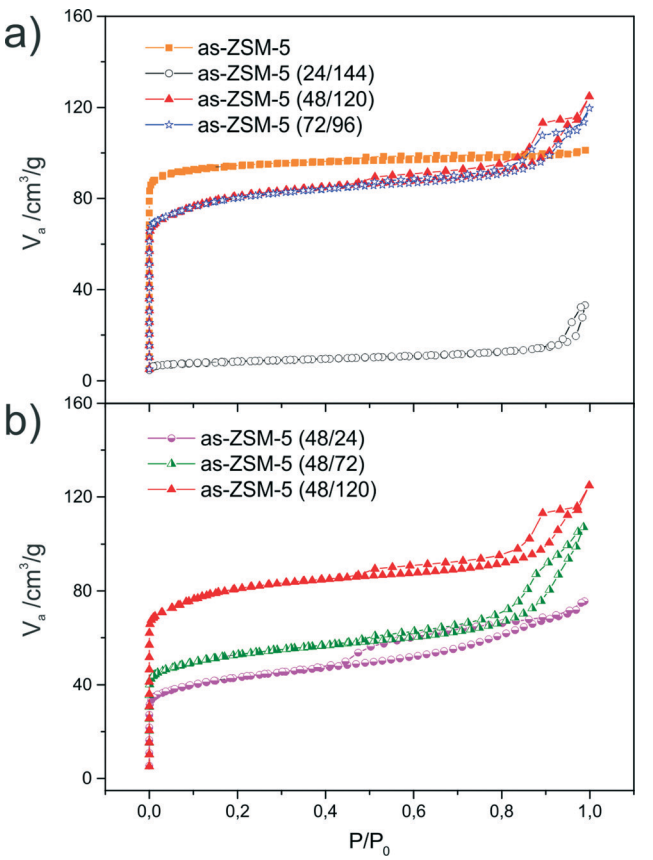

Fig. 1 Nitrogen adsorption–desorption isotherms of the as-synthesized samples aged for different times before (a) and after (b) acidification.

The XRD powder patterns of the as-synthesized samples are shown in Fig. 2. A diffractogram of as-ZSM-5 (Fig. 2a) contains all reflections characteristic of the MFI topology,[27] which proves the successful synthesis of the parent zeolite. The synthesis modification through acidification resulted in a decrease of the reflection intensity. In the cases of as-ZSM-5 (48/120) and as-ZSM-5 (72/96) the structure of the MFI topology was preserved, however, in the case of as-ZSM-5 (24/144), a broad reflection at about 2θ values of 15–30°, assigned to amorphous silica,[12] was found. For this sample, only low-intensity reflections characteristic of the ZSM-5 structure were identified. These results are in agreement with the N_2 sorption studies and prove that 24 h of zeolite parent mixture crystallization before acidification was not enough to create the MFI structure. Instead of the MFI structure, amorphous material was formed. Fig. 2b shows diffractograms of the samples aged for 48 h before acidification and for different aging durations (24, 72 and 120 h) after acidification. A decrease in the reflection intensities for the samples with decreased crystallization times after acidification was observed. Thus, it could be concluded that the aging stage after acidification also influences the final crystallinity of hierarchical zeolites.

The degree of microporous structure formation during synthesis of the hierarchical materials can be specified by thermal analysis. The DTG profiles of the as-synthesized samples are presented in Fig. 3. The DTG curve obtained for as-ZSM-5 (Fig. 3a) consists of three regions of weight loss.[30–32] The first region, at temperatures below 100 °C, is assigned to the desorption of zeolitic water, while the second (100–300 °C) and third (>300 °C) regions are related to the decomposition of the structure directing agent (TPAOH), balancing the charge of $Si\text{-}O^-$ groups in the connectivity defects and $Al(OSi)_4^-$ within the various types of micropores, respectively. In the DTG curve of as-ZSM-5 (24/144), the high temperature peaks connected with TPAOH decomposition occluded within the micropore structure are not present. Additionally, in the DTG profile obtained for this sample, a small peak at about 100 °C, probably connected with the decomposition of organic surfactant present on the surface of the amorphous material, was detected.

These results, which are in agreement with the N_2 sorption and XRD analyses, proved that 24 h of hydrothermal crystallization of ZSM-5 synthesis gel before acidification was not enough to form the MFI zeolitic structure. In the case of the samples aged for 48 and 72 h (as-ZSM-5 (48/120) and as-ZSM-5 (72/96)), the weight loss observed in the second region is more intensive than for the conventional as-ZSM-5 zeolite. However, the peaks in the third region are less intense and are also shifted to lower temperatures. These changes could be related to the shorter crystallization time of the zeolitic phase in case of the micro-mesoporous samples, that results in weaker incorporation of TPA^+ within the zeolite structure (weaker stabilization in the pore system). In the case of the series differing in aging duration after acidification (Fig. 3b), lower stability of organic surfactants within the micropore structure with decreasing aging duration was observed. An intensive peak at about 210 °C, assigned to TPA^+ balancing the connectivity defects in the structure of the micro-mesoporous as-ZSM-5 (48/120) sample, decreased after shortening of the aging duration from 120 to 72 h and disappeared after shortening of this procedure to 24 h. In the case of as-ZSM-5 (48/24), this change was connected with the appearance of a small peak at about 100 °C (the same as in the case of

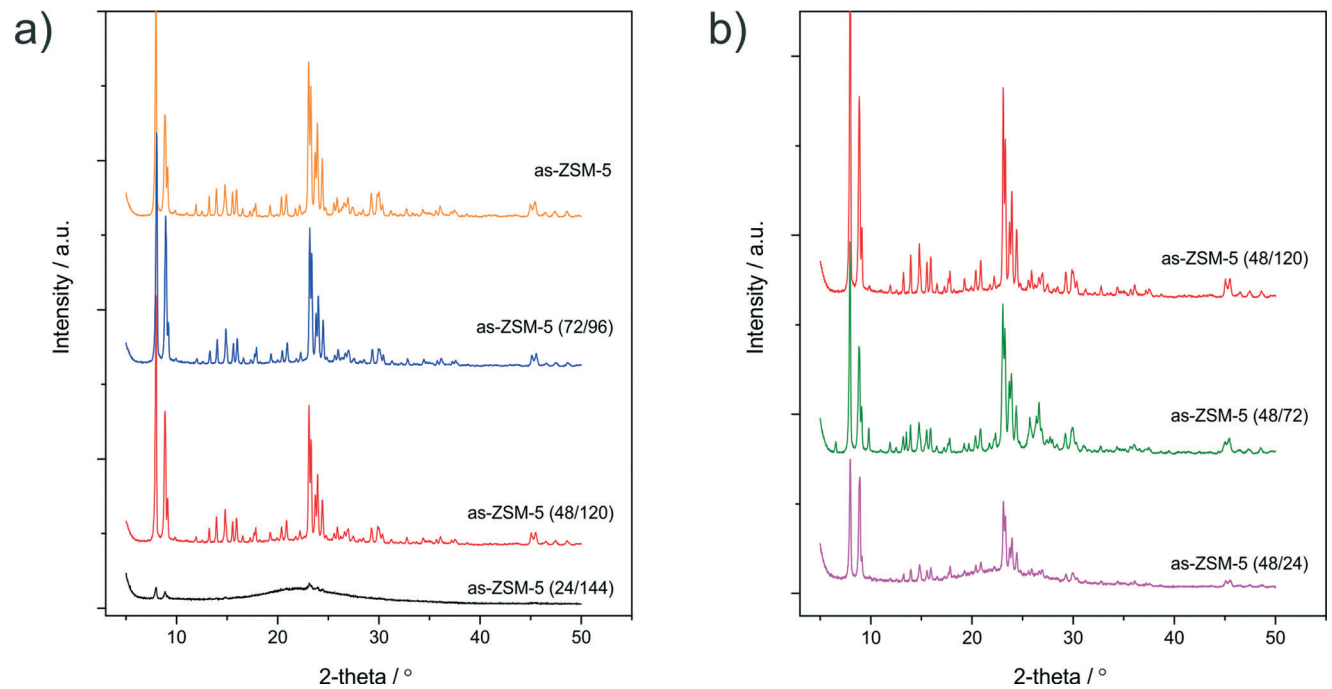

Fig. 2 XRD patterns of the as-synthesized samples aged for different times before (a) and after (b) acidification.

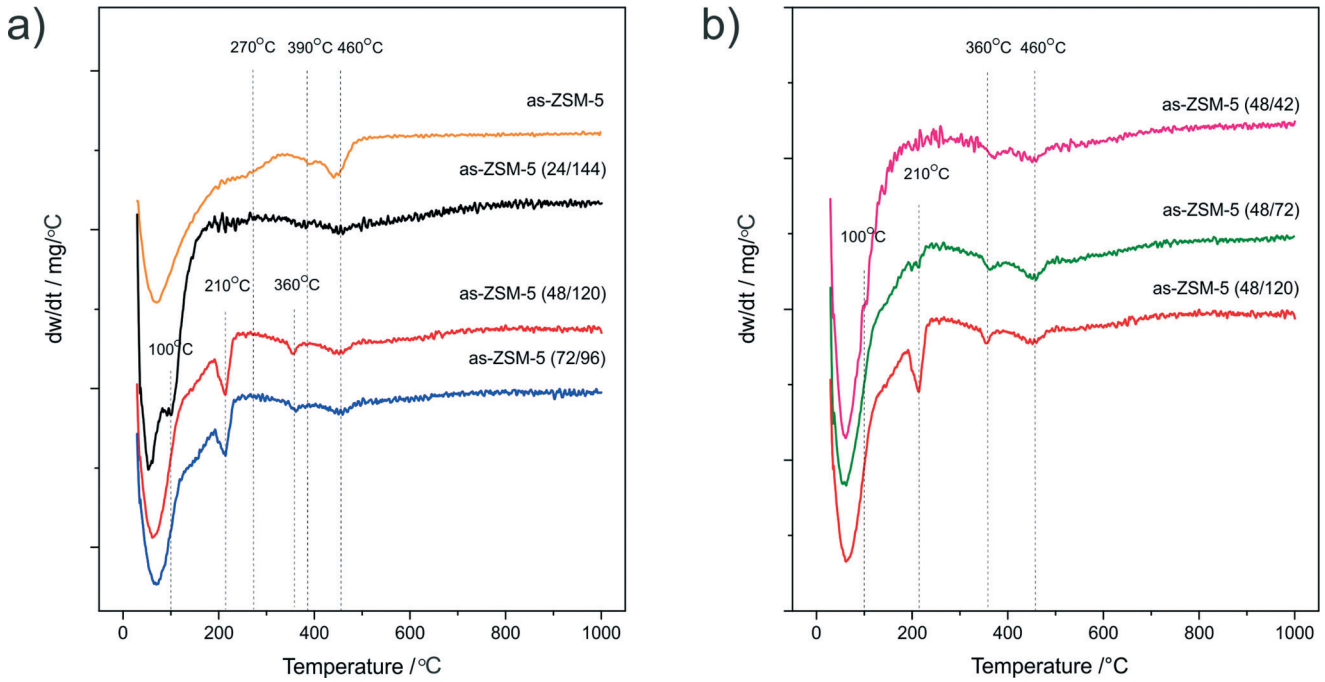

Fig. 3 DTG profiles of the as-synthesized samples aged for different times before (a) and after (b) acidification.

as-ZSM-5 (24/144)), probably related to combustion of TPAOH not interacting with the zeolite matrix.

The Si/Al ratios in the as-synthesized samples were analyzed using the atomic absorption spectroscopy (AAS) method (Table 2). The relatively low Si/Al ratio, equal to 12 in the case of as-ZSM-5, increased after modification of the porous structure by acidification. The lower Al content in the micro-mesoporous samples can be connected with disturbed and incomplete crystallization of the samples. However, a clear dependency between the duration of zeolite hydrothermal aging and changes in the Si/Al ratio was not observed. Therefore, it could be concluded that the acidification of the samples with a total duration of hydrothermal aging of 7 days increased the Si/Al ratio to about 20, and the shortening of the aging duration after acidification increased this ratio to about 35. Thus, both the factors of acidification and shortening of the crystallization time influenced the Al content in the modified samples.

Temperature-programmed desorption of ammonia (NH_3-TPD) was used to determine the surface acidity (surface concentration and strength of acid sites) of the as-synthesized samples and their protonic forms (after triple ion-exchange with NH_4NO_3 followed by calcination). The surface concentration of acid sites (Table 3) was calculated by the integration of areas under TPD profiles, which were recalculated into a number of adsorbed ammonia molecules (it was assumed that one NH_3 molecule adsorbs on one acid site). The total NH_3 uptake obtained in the case of as-ZSM-5, equal to 819 μmol g^{-1}, decreased after modification by acidification of the synthesis gel. This effect could be explained by the shorter hydrothermal aging time and acidification of the hierarchical samples, which disturbed crystallization of the samples and thus resulted in lower amount of framework Al. In the case of the samples aged for 48 and 72 h (as-ZSM-5 (48/120) and as-ZSM-5 (72/96)) the concentrations of acid sites were equal to 322 and 439, respectively, while in the case of as-ZSM-5 (24/144), a significant decrease in this value (26 μmol g^{-1}) was observed. Taking into account the similar Si/Al ratio determined for all three samples by the AAS method, it could be supposed that a substantial part of Al was present in as-ZSM-5 (24/144) in the amorphous and low-surface phase. Shortening of the crystallization time after acidification

Table 3 Concentration of acid sites measured by NH_3 sorption for the as-synthesized samples and their H-forms

Sample code	NH_3 uptake/μmol g^{-1}	Sample code	NH_3 uptake/μmol g^{-1}
as-ZSM-5	819	H-ZSM-5	925
as-ZSM-5 (24/144)	26	H-ZSM-5 (24)	29
as-ZSM-5 (48/120)	322	H-ZSM-5 (48)	325
as-ZSM-5 (72/96)	439	H-ZSM-5 (72)	420
as-ZSM-5 (48/24)	149	H-ZSM-5 (48/24)	198
as-ZSM-5 (48/72)	190	H-ZSM-5 (48/72)	209
		H-ZSM-5/H_2O	235
		H-ZSM-5 (48/120)/H_2O	87

additionally decreased the concentration of acid sites, which is in agreement with the AAS results.

The increase in surface acidity, observed after ion-exchange in the majority of the samples, is possibly related to the formation of acid Brønsted sites, as structural ≡Al–O(H)–Si≡ groups of the zeolite framework.

NH_3-TPD profiles of the as-synthesized samples and their H-forms (beside as-ZSM-5 (24/144) and H-ZSM-5 (24/144), with a very low surface density of acid sites) are presented in Fig. 4a and b, respectively. In the obtained NH_3-TPD profiles, three types of acid sites, with respect to their acidic strength, can be distinguished: (i) at about 200 °C, attributed to weak acid sites, so called α sites, (ii) at about 300 °C, attributed to medium acid sites, so called β sites, and (iii) at about 400 °C, attributed to strong acid sites, so called γ sites.[33,34] The shape of the ammonia desorption profile significantly changed after modification of the porous structure by acidification (Fig. 4a). The changes observed after acidification of the zeolite seeds solution can be connected with partial protonation of the micro-mesoporous samples (using HCl), while in the case of the conventional as-ZSM-5 sample directly after synthesis, the Na-form was obtained.

After ion-exchange to obtain H-forms of the micro-mesoporous samples, the shapes of the NH_3 desorption profiles were not changed significantly (only a slight increase in desorption spectra intensity was observed), while in the case of conventional, microporous ZSM-5, the changes were much more significant. After ion-exchange of the samples with NH_4NO_3, the peak corresponding to β-type acid sites disappeared in favor of a high temperature peak at about 400–500 °C (γ-type acid sites). The obtained results suggest that by exchange of Na^+ for H^+, the β-type acid sites, which are possibly Lewis type sites, were turned into γ-type, which are probably Brønsted acid sites.[33]

It is also worth noticing that despite the presence of α- and γ-types of acid sites in all the H-form samples, the peaks present in the TPD profile of H-ZSM-5 are shifted to higher temperatures in comparison to the micro-mesoporous samples. This means that the structural disorder caused by acidification results in acid sites of slightly lower strength in comparison to the conventional zeolite.

Bright field transmission electron microscopy (BFTEM) images (Fig. 5) of two selected samples (as-ZSM-5 and as-ZSM-5 (48/120)) give an overview of the conventional and micro-mesoporous materials morphology. The structures of the conventional ZSM-5 and the acidified sample differ significantly. In the case of the micro-mesoporous sample, zeolite seeds, formed during hydrothermal treatment before acidification, were aggregated (during hydrothermal treatment after acidification) with the formation of a loose, wormhole like structure. The mesoporosity in the as-ZSM-5 (48/120) sample was generated between the zeolitic seeds with sizes of 10–20 nm. A similar morphology of the micro-mesoporous samples was obtained in the case of hierarchical Beta zeolite synthesized using the same method (meso-template-free method).[12,14,15] In both the samples, the aluminum distribution determined by EDX analysis was uniform (results not shown).

3.2. Catalytic study: MTD reaction

Results of the catalytic studies of the as-synthesized samples and their H-forms in the process of DME synthesis from methanol are presented in Fig. 6 and 7, respectively. The methanol conversion over the as-synthesized micro-mesoporous samples (Fig. 6a) increased with increasing aging duration before acidification. The catalytic activity of as-ZSM-5 (48/120) and as-ZSM-5 (72/96) did not differ significantly, which is a result of the similar physicochemical properties of these samples. Maximum methanol conversion in the presence of these samples was obtained at 225 °C. A further temperature increase resulted in a slight decrease in methanol conversion, which can be explained by the exothermic character of this reaction.[24,26] A significant increase in catalytic activity related to the prolongation of the aging duration before acidification from 24 to 48 h can be connected with a substantial increase in the surface density of acid sites (acid sites are most likely considered as active centers of DME synthesis). The changes in methanol conversion observed for the catalysts obtained with an increasing duration of hydrothermal treatment was accompanied by a decrease in the reaction selectivity towards DME (only at high temperatures). High acidity of the samples is from one side responsible for the catalytic efficiency of methanol conversion, however, on the other side, this is a cause of by-product formation. The as-ZSM-5 sample, despite having the highest concentration of acid sites among the examined samples, was completely inactive in methanol conversion. This result suggests that not only the concentration of acid sites, but also their strength (the NH_3-TPD profile of this sample significantly differs from those obtained for other samples in this series) is essential in DME synthesis from methanol. The shortening of the aging duration after acidification (Fig. 6b) slightly decreased methanol conversion and increased the selectivity towards DME. This effect can be associated with a decrease in the surface density of acid sites observed for the samples with shortened hydrothermal treatment after acidification.

The most significant changes in the catalytic activity of the samples after ion-exchange to H-form were observed in the case of the H-ZSM-5 sample (Fig. 7a). The as-ZSM-5 catalyst, which was completely inactive, showed the highest methanol conversion after ion-exchange to its H-form among the examined samples. Thus, it could be concluded that strong acid sites of γ-type are responsible for methanol dehydration to DME. On the other hand, the presence of the strong acid sites in H-ZSM-5 decreased the reaction selectivity towards DME. Dimethyl ether was not detected in the outlet gases at temperatures about 25 °C lower in comparison to the reaction performed in the presence of the hierarchical samples.

In the case of the samples aged for different times after acidification (Fig. 7b) ion-exchange to their H-forms resulted

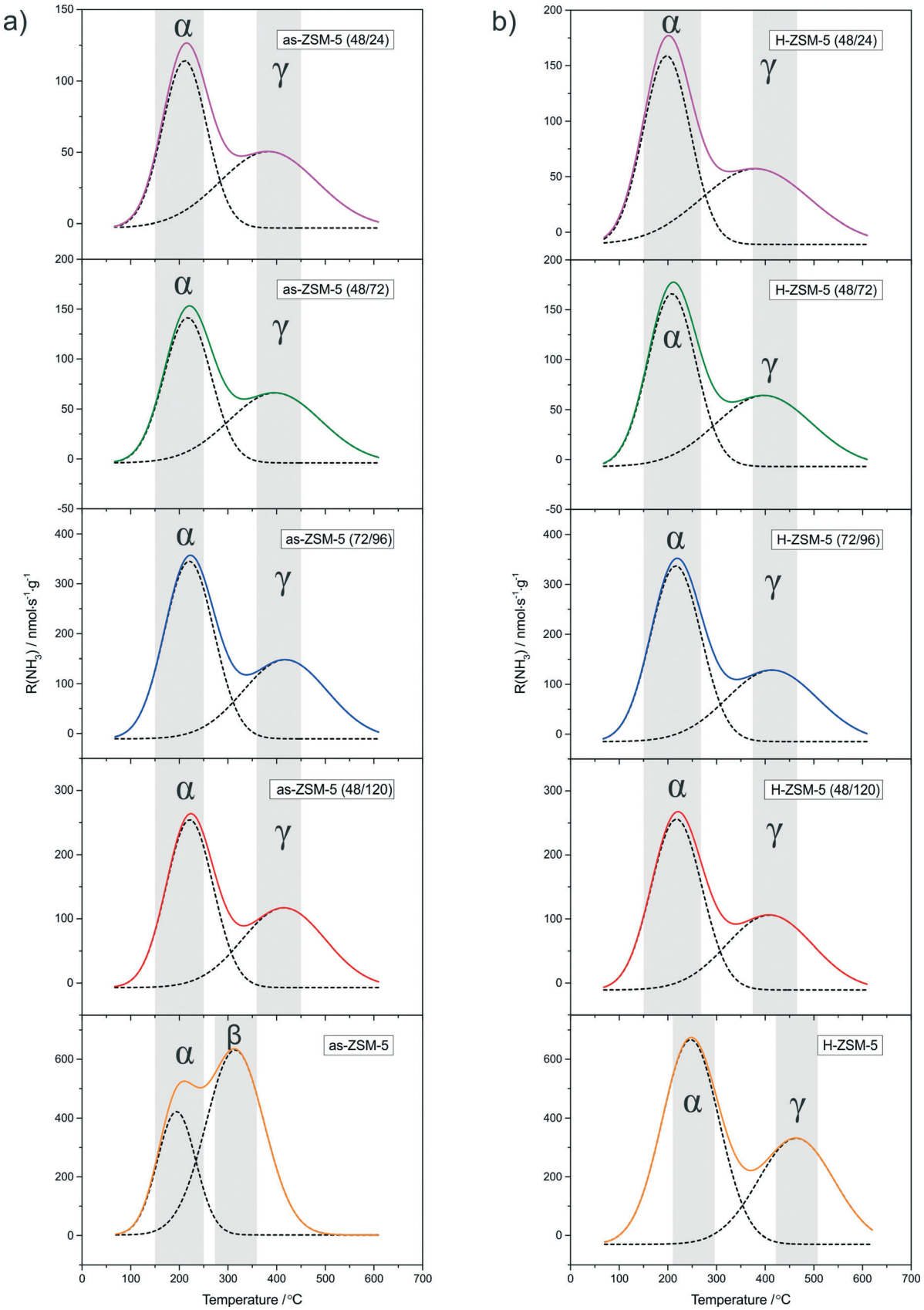

Fig. 4 NH_3-TPD profiles of the as-synthesized samples (a) and their H-forms (b). Conditions: 10 000 ppm NH_3 in He; gas flow 20 ml min^{-1}; weight of catalyst = 0.05 g.

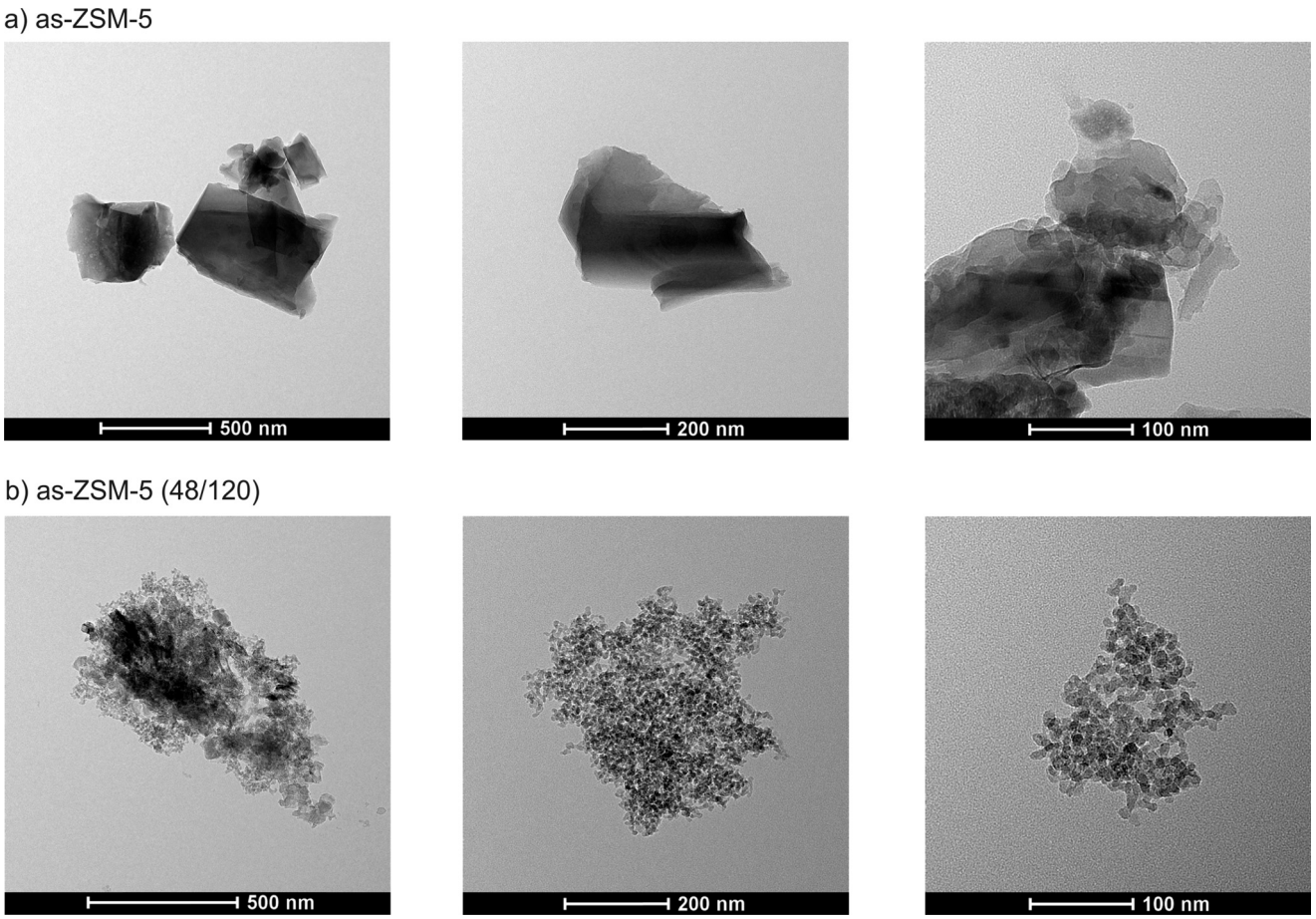

Fig. 5 BFTEM images of conventional as-ZSM-5 zeolite (a) and the micro-mesoporous as-ZSM-5 (48/120) sample (b) with different magnifications.

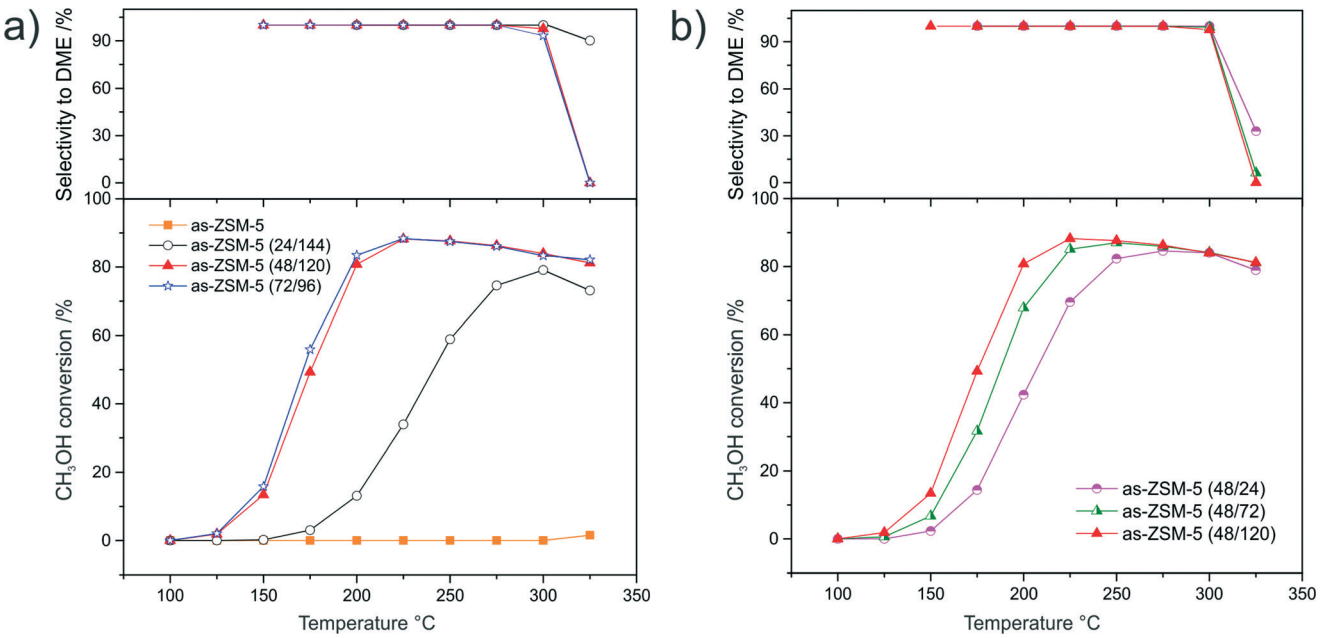

Fig. 6 Temperature dependence of CH_3OH conversion and selectivity towards DME over the as-synthesized samples aged for different times before (a) and after (b) acidification. Conditions: 4 vol% CH_3OH; He as balancing gas; total flow rate = 20 ml min^{-1}; weight of catalyst = 0.1 g.

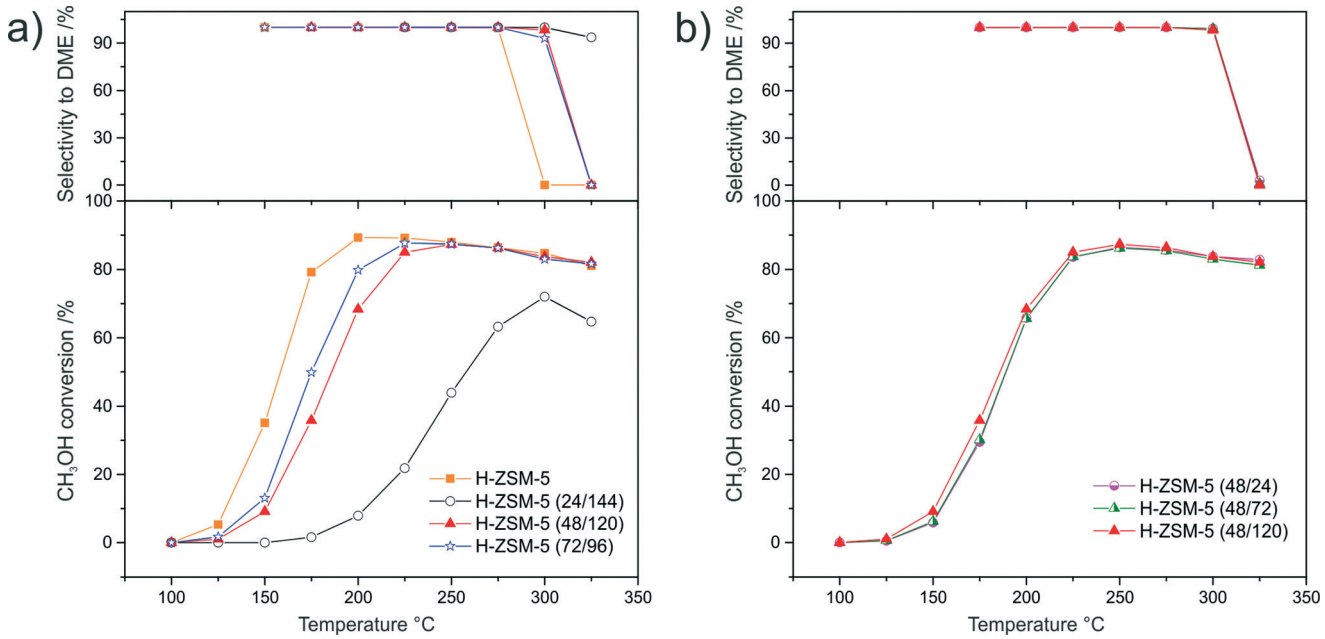

Fig. 7 Temperature dependence of CH_3OH conversion and selectivity towards DME over H-forms of the samples aged for different times before (a) and after (b) acidification. Conditions: 4 vol% CH_3OH; He as balancing gas; total flow rate = 20 ml min^{-1}; weight of catalyst = 0.1 g.

in a very similar activities in methanol conversion and selectivity towards DME for all three samples (H-ZSM-5 (48/120), H-ZSM-5 (48/24) and H-ZSM-5 (48/72)). This was connected with the increased acidity of H-ZSM-5 (48/24) and H-ZSM-5 (48/72) after ion-exchange with NH_4NO_3. Thus, it could be concluded that the change in duration of hydrothermal treatment after acidification did not influence the catalytic activity of the samples in the process of DME synthesis.

It should be also stressed that the relatively high activity of the hierarchical samples was obtained directly after synthesis (as-form of the samples), while in the case of as-ZSM-5, an additional synthesis step was needed for the activation of this sample in the considered catalytic reaction.

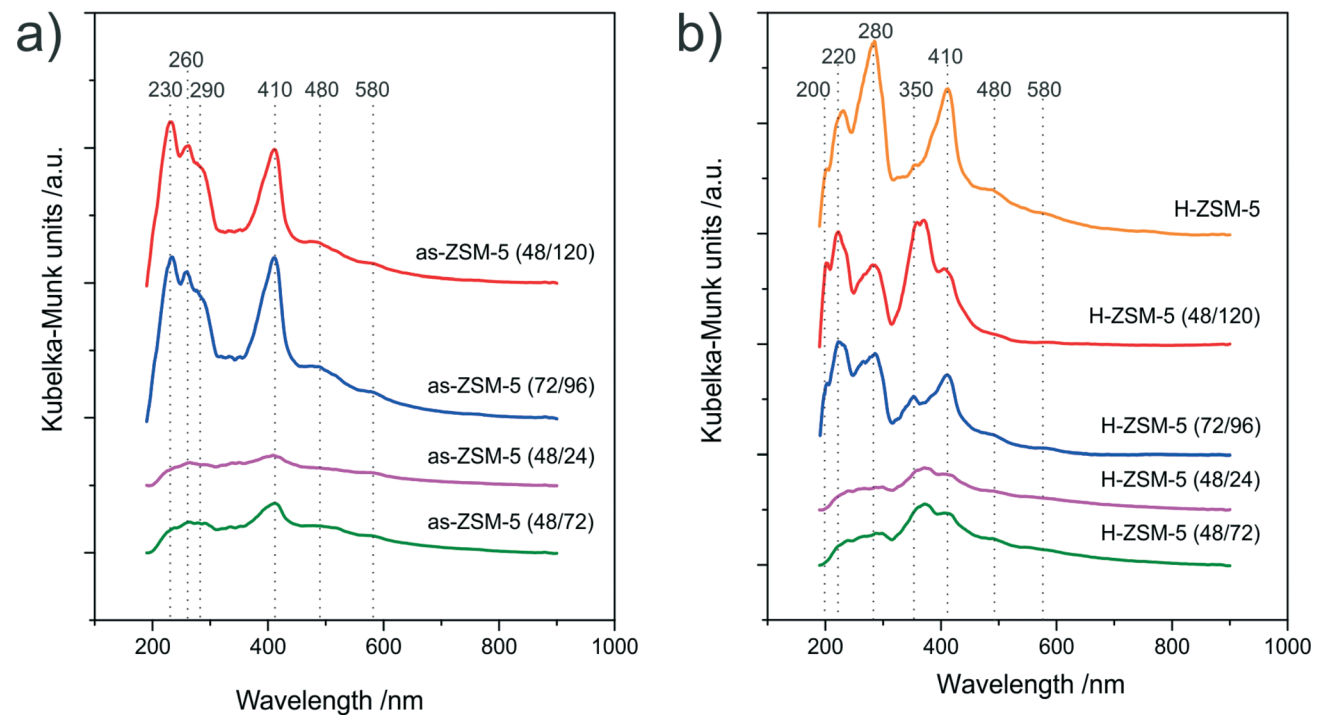

Fig. 8 UV-vis difference spectra of carbon deposits formed during catalytic reaction of the as-synthesized samples (a) and their H-forms (b).

Methanol conversion resulted not only in the formation of the desired DME but also side products (polyolefins, aromatic compounds and carbon deposits) responsible for the gradual deactivation of the catalysts by the blocking of active sites. Moreover, during the aging of such deposits (growth of polycyclic aromatic structures), the zeolite pore system can be blocked, which decreases the efficiency of the internal diffusion of reactants.[35] The chemical nature of the formed coke deposit was analyzed using a UV-vis-DRS technique. Fig. 8a and b show the UV-vis-DR spectra obtained for the as-synthesized samples and their H-forms after the catalytic tests (only for the samples in which coke deposits were formed) for methanol conversion, respectively. In case of the as-synthesized samples (Fig. 8a) six absorption bands with different intensities were identified. The bands in the first region (200–300 nm) may be ascribed to dienes, cyclohexadiene, benzene or substituted benzenes. While the bands in the second region (400–600 nm) can be attributed to bulky aromatic species, like diphenyl, polyphenyl carbenium ions, polyalkyloaromatics or condensated aromatic ring systems.[36,37]

The intensity of these bands increased together with an increase in the sample acidity. The conversion of zeolites to their H-forms by ion-exchange resulted in the formation of new bands in the UV-vis-DR spectra, which proves the more complex structure of carbon deposits (greater heterogeneity of coke species). This is probably related to the enhanced Brønsted acidity of the samples.

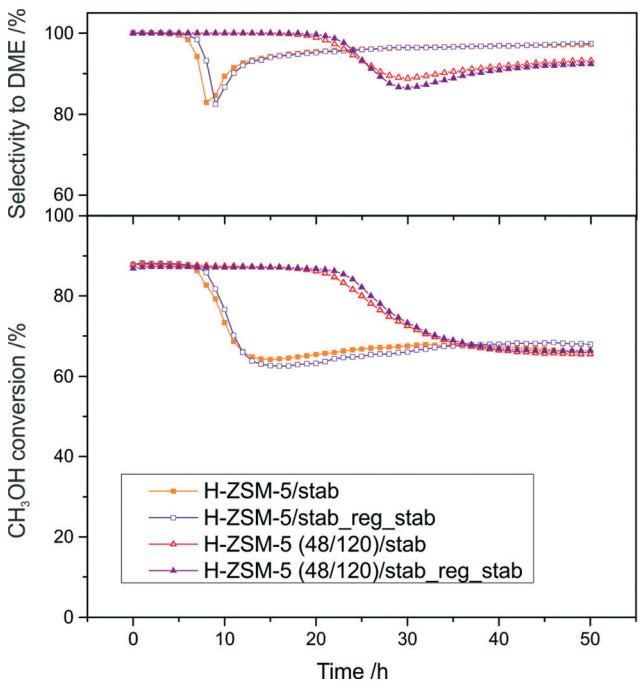

Fig. 9 Time dependence (stability tests: 50 h at 250 °C before and after regeneration) of CH_3OH conversion and selectivity to DME of H-ZSM-5 and H-ZSM-5 (48/120). Conditions: 4 vol% CH_3OH; He as balancing gas; total flow rate = 20 ml min^{-1}; weight of catalyst = 0.1 g.

Fig. 9 shows the results of stability tests (50 h of continuous work at 250 °C) for two selected catalysts – the parent H-ZSM-5 and micro-mesoporous H-ZSM-5 (48/120) (the temperature of the stability tests was adjusted to analyze the catalyst stability for a methanol conversion of about 90%). After the stability test, the samples H-ZSM-5/stab and H-ZSM-5 (48/120)/stab were regenerated (oxidation of carbon deposit in a flow of oxygen (5% in He, 20 ml min^{-1}) at 600 °C with QMS detection of 44 line (CO_2)) and examined in a stability test for the second time (H-ZSM-5/stab_reg_stab and H-ZSM-5 (48/120)/stab_reg_stab).

The methanol conversion in the presence of parent H-ZSM-5 decreased by about 30% after 10 h of time on stream and subsequently stabilized at about 70%. In case of the hierarchical sample, the methanol conversion remained at a constant level for a longer time on stream than the conventional zeolite. After 20 h of continuous work, the methanol conversion started to progressively drop to about 70%. The changes in catalyst activity were accompanied by changes in the reaction selectivity towards DME. In the case of H-ZSM-5, a sharp decline in selectivity towards DME after 10 h of the stability test, which subsequently progressively increased to about 97%, was observed. In the case of H-ZSM-5 (48/120), selectivity towards DME started to decrease after 20 h of time on stream and stabilized at about 92% after 50 h of the stability test. It could be concluded that during the first few hours of the stability test, better results were obtained for the hierarchical sample. It is possible that the presence of stronger acid sites in the case of conventional ZSM-5 zeolite was a cause of their faster deactivation by coke formation (sharp drop of activity and selectivity after 10 h). After full coverage (deactivation) of the strongest acid sites, the reaction started to proceed on other acid sites, with strengths comparable to those present in the micro-mesoporous sample. This resulted in re-growth of the selectivity towards DME and a decrease in methanol conversion (lower acidity of the sample). In the case of the micro-mesoporous sample (H-ZSM-5 (48/120)), the acid sites of lower strength (in comparison to the conventional zeolite) were deactivated by coke deposits after a longer time in the stability test (a shift of about 20 h). It is also possible that the presence of mesopores prolonged the access to the active sites, which were easily blocked in the cases involving poorly microporous materials. It is important to notice that both the conversion and selectivity profiles (in the case of both the examined samples) were not changed significantly after regeneration, which proves their shape dependence only on the formation of coke deposits. The X-ray diffraction patterns of the samples after the stability tests were not changed significantly (Fig. 10). In both cases, practically all (*hkl*) reflections remained unchanged and only their slight broadening and decreased intensities were observed, proving the preservation of the zeolite structure. The textural parameters of the spent samples determined by N_2 sorption (samples outgassed before measurement at 50 °C) differ significantly. The BET surface area and surface area and volume of micropores decreased in case of both the samples, however this effect

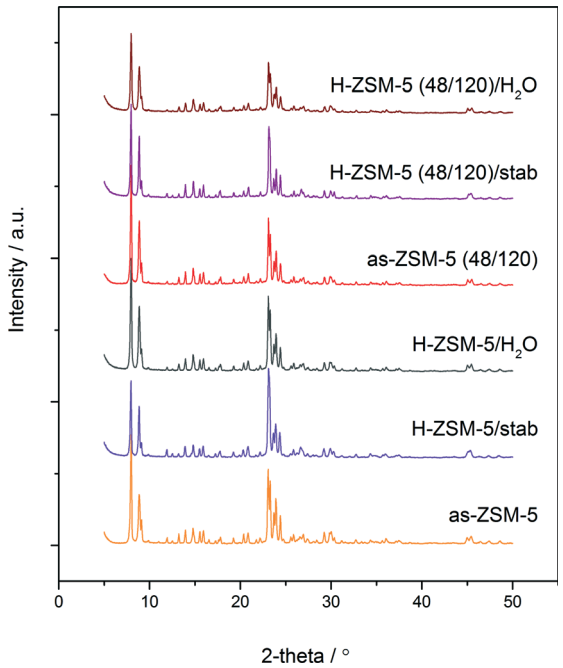

Fig. 10 XRD patterns of fresh and spent (after 50 h stability test at 250 °C and after 2 h hydrothermal test at 250 °C/6 h + H_2O) conventional ZSM-5 and micro-mesoporous ZSM-5 (48/120).

was much more significant in case of the conventional ZSM-5 zeolite (Table 2). These results point out the significant blocking of micropores by coke deposit, which in a great expense decreased the accessibility of the active sites on the catalyst surface. This phenomenon was limited in the case of the micro-mesoporous sample.

The chemical nature of the carbon deposits formed during the stability test (samples marked as H-ZSM-5/stab and H-ZSM-5 (48/120)/stab) was analyzed by two experimental methods – UV-vis-DR spectroscopy and thermogravimetric analysis coupled with QMS detection of gas products (Fig. 11a and b respectively). In the case of H-ZSM-5/stab (Fig. 11a), the spectrum contains more bands than the spectrum of the hierarchical sample (H-ZSM-5 (48/120)/stab), which is evidence of the higher heterogeneity of the coke deposits. Moreover, the intensity of the bands in the spectrum of the conventional zeolite is greater in comparison to the micro-mesoporous sample, especially at higher wavelengths. This proves the presence of polycondensed aromatics of higher condensation. Only one band in the spectra of H-ZSM-5 (48/120)/stab, located at about 370 nm and attributed to conjugated double bonds and polycondensed aromatics,[37] is characterized by a higher intensity.

In both the samples, evolution of CO_2 (Fig. 11b) at a relatively low temperature as well as evolution of water vapour in the same temperature range (m/z = 18) (results not shown) suggests that the formed coke deposits, apart from carbon, also contain hydrogen. For the H-ZSM-5/stab sample, the evolution of a higher amount of CO_2 was detected. The weight loss connected with the burning of carbon deposits, measured in the case of this sample, was equal to about 6.5%, while in the case of the hierarchical sample, this was 2.5%. For both the samples, two peaks of CO_2 evolution were identified. These peaks can be related to the different nature of the formed coke. The first peak, at about 340 °C, can be attributed to slightly developed coke, while the second one, at about 510 °C, can be attributed to its more condensed forms (with a lower H/C ratio).[38]

In order to verify the hydrothermal stability of the samples, H-ZSM-5 and H-ZSM-5 (48/120) were treated in a water vapor atmosphere (~3% H_2O) at 250 °C for 6 h. The comparison of the catalytic activity before and after treatment in the water vapor atmosphere (2 h stability tests at 250 °C) is presented in Fig. 12. The treatment of the micro-mesoporous sample in such conditions resulted in a significant decrease in its activity (by about 50%), while the activity of the conventional zeolite practically was not changed (selectivity towards DME in case of both the samples before and after hydrothermal treatment was 100%, results not shown). The physicochemical properties of the samples after hydrothermal

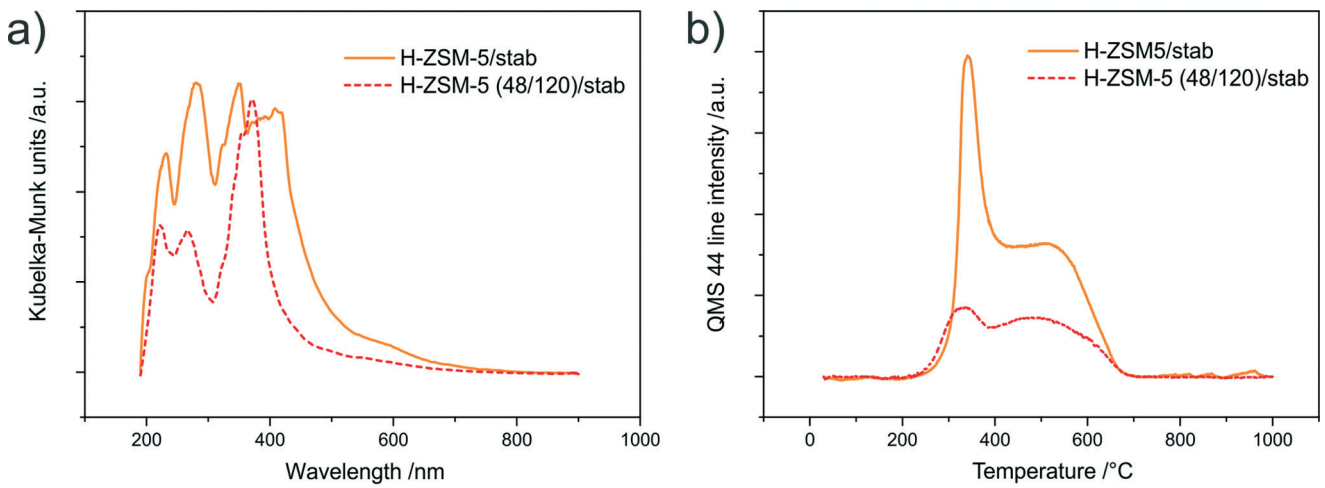

Fig. 11 UV-vis difference spectra of carbon deposits (a) and CO_2 evolution signals measured by QMS of the samples after the stability test.

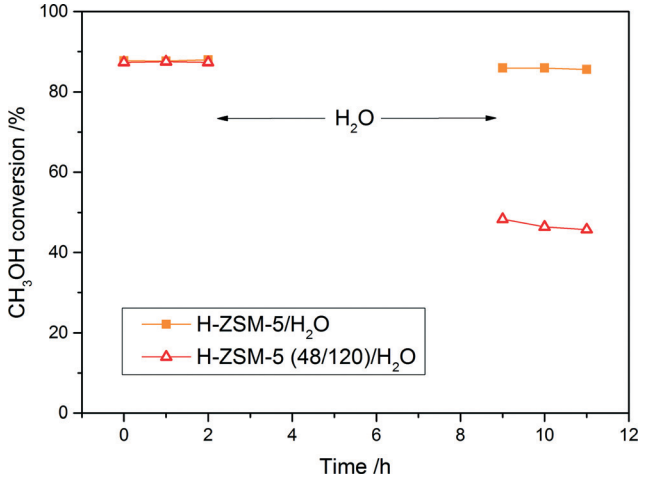

Fig. 12 Time dependence (hydrothermal stability tests: 2 h at 250 °C/6 h at 250 °C +H_2O/2 h at 250 °C) of CH_3OH conversion of H-ZSM-5 and H-ZSM-5 (48/120). Conditions: 4 vol% CH_3OH/3% H_2O; He as balancing gas; total flow rate = 20 ml min^{-1}; weight of catalyst = 0.1 g.

treatment were examined by X-ray diffraction (Fig. 10), low temperature N_2 sorption (Table 2) and NH_3-TPD (Table 3) methods. The obtained XRD diffractograms indicated the preservation of the crystalline MFI structure of the samples, however a decrease in the textural properties and acidity (especially in the case of the micro-mesoporous sample) was observed. It seems that during the hydrothermal treatment of the samples, the collapse of porous structure and steam assisted dealumination could occur. The obtained conversion after hydrothermal treatment is comparable with the other samples in this series with similar concentrations of acid sites.

It is worth noticing that the lowered resistance to the hydrothermal conditions in case of the micro-mesoporous sample was observed under severe conditions (resulting in a complete catalyst deactivation), while during a much longer stability test under reaction conditions, it behaved similar to conventional ZSM-5.

Conclusions

In the frame of the undertaken studies, a new method for the synthesis of micro-mesoporous materials with ZSM-5 properties was developed. The obtained samples were studied to investigate the role of the catalysts for the synthesis of DME from methanol. The catalytic performance of the zeolitic samples was correlated with their properties – porosity, acidity and crystallinity.

Two parameters – the duration of the hydrothermal treatment (i) before and (ii) after acidification were selected as parameters for the synthesis optimization leading to effective catalysts for DME production.

The obtained results lead to the conclusion that the optimal durations of synthesis gel aging before and after acidification are equal to 48 and 120 h, respectively. Nano-seeds of ZSM-5 zeolite are created during the first 48 h of hydrothermal treatment of the synthesis mixture and prolongation of this time does not influence significantly the physicochemical properties of the samples. The duration of aging after modification also strongly influences the textural parameters, acidity and crystallinity of the samples, which proved that both stages of hydrothermal treatment have a strong impact on the final properties of the samples.

It was confirmed that the high catalytic efficiency in the synthesis of DME is connected with the presence of strong acid sites of γ-type (acid sites of Brønsted type). The as-synthesized micro-mesoporous samples showed high catalytic activity (similar to conventional ZSM-5), however the presence of weaker acid sites in their structure, connected with generated mesoporosity, resulted in improved reaction selectivity towards DME.

Results of the stability tests (50 h on stream) performed for H-ZSM-5 and H-ZSM-5 (48/120), as well as the analysis of the spent catalysts, showed that the sample with the hierarchical porous structure was more stable (especially during the first few hours of the stability test) and was more resistant to carbon deposit formation.

Acknowledgements

This work was supported by the National Science Center under grant no. 2011/03/N/ST5/04820. Part of the research was carried out with equipment purchased thanks to the financial support of the European Regional Development Fund in the framework of the Polish Innovation Economy Operational Program (contract no. POIG.02.01.00-12-023/08). U. D. gives thanks to Spanish Government by the funding (project MAT2014-52085-C2-1-P).

Notes and references

1 D. Verboekend and J. Pérez-Ramírez, *Catal. Sci. Technol.*, 2011, **1**, 879.
2 D. Verboekend and J. Pérez-Ramírez, *Chem. – Eur. J.*, 2011, **17**, 1137.
3 L. Jin, H. Hu, S. Zhu and B. Ma, *Catal. Today*, 2010, **149**, 207.
4 L. H. Ong, M. Dömök, R. Olindo, A. C. van Veen and J. A. Lercher, *Microporous Mesoporous Mater.*, 2012, **164**, 9.
5 J.-B. Koo, N. Jiang, S. Saravanamurugan, M. Bejblová, Z. Musilová, J. Čejka and S.-E. Park, *J. Catal.*, 2010, **276**, 327.
6 L. Wang, Z. Zhang, C. Yin, Z. Shan and F.-S. Xiao, *Microporous Mesoporous Mater.*, 2010, **131**, 58.
7 Y. Zhu, Z. Hua, J. Zhou, L. Wang, J. Zhao, Y. Gong, W. Wu, M. Ruan and J. Shi, *Chem. – Eur. J.*, 2011, **17**, 14618.
8 M. Choi, K. Na, J. Kim, Y. Sakamoto, O. Terasaki and R. Ryoo, *Nature*, 2009, **461**, 246.
9 K. Na, M. Choi, W. Park, Y. Sakamoto, O. Terasaki and R. Ryoo, *J. Am. Chem. Soc.*, 2010, **132**, 4169.
10 X. Zhang, D. Liu, D. Xu, S. Asahina, K. A. Cychosz, K. Varoon Agrawal, Y. Al Wahedi, A. Bhan, S. Al Hashimi, O. Terasaki, M. Thommes and M. Tsapatsis, *Science*, 2012, **336**, 1684.
11 L. Tosheva and V. P. Valtchev, *Chem. Mater.*, 2005, **17**(10), 2494.

12 M. Rutkowska, L. Chmielarz, D. Macina, Z. Piwowarska, B. Dudek, A. Adamski, S. Witkowski, Z. Sojka, L. Obalová, C. J. Van Oers and P. Cool, *Appl. Catal., B*, 2014, **146**, 112.
13 M. Rutkowska, Z. Piwowarska, E. Micek and L. Chmielarz, *Microporous Mesoporous Mater.*, 2015, **209**, 54.
14 C. J. Van Oers, W. J. J. Stevens, E. Bruijn, M. Mertens, O. I. Lebedev, G. Van Tendeloo, V. Meynen and P. Cool, *Microporous Mesoporous Mater.*, 2009, **120**, 29.
15 C. J. Van Oers, M. Kurttepeli, M. Mertens, S. Bals, V. Meynen and P. Cool, *Microporous Mesoporous Mater.*, 2014, **185**, 204.
16 J. Sun, G. Yang, Y. Yoneyama and N. Tsubaki, *ACS Catal.*, 2014, **4**, 3346.
17 Z. Azizi, M. Rezaeimanesh, T. Tohidian and M. R. Rahimpour, *Chem. Eng. Process.*, 2014, **82**, 150.
18 S. Hassanpour and M. Taghizadeh, *Ind. Eng. Chem. Res.*, 2010, **49**, 4063.
19 A. A. Rownaghi, F. Rezaei, M. Stante and J. Hedlund, *Appl. Catal., B*, 2012, **119-120**, 56.
20 G. Laugel, X. Nitsch, F. Ocampo and B. Louis, *Appl. Catal., A*, 2011, **402**, 139.
21 M. Rutkowska, D. Macina, N. Mirocha-Kubień, Z. Piwowarska and L. Chmielarz, *Appl. Catal., B*, 2015, **174**, 336.
22 Y. Wei, P. E. de Jongh, M. L. M. Bonati, D. J. Law, G. J. Sunley and K. P. de Jong, *Appl. Catal., A*, 2015, **504**, 211.
23 Q. Yang, H. Zhang, M. Kong, X. Bao, J. Fei and X. Zheng, *Chin. J. Catal.*, 2013, **34**, 1576.
24 H. Li, S. He, K. Ma, Q. Wu, Q. Jiao and K. Sun, *Appl. Catal., A*, 2013, **450**, 152.
25 Y. Sang, H. Liu, S. He, H. Li, Q. Jiao, Q. Wu and K. Sun, *J. Energy Chem.*, 2013, **22**, 769.
26 Q. Tang, H. Xu, Y. Zheng, J. Wang, H. Li and J. Zhang, *Appl. Catal., A*, 2012, **413-414**, 36.
27 H. Robson and K. P. Lillerud, *Verified Synthesis of Zeolitic Materials*, Elsvier, 2001, ISBN: 0-444-50703-5.
28 J. Rouquerol, P. Llewellyn and F. Rouquerol, *Stud. Surf. Sci. Catal.*, 2007, **160**, 49.
29 M. Thommes, K. Kaneko, A. V. Neimark, J. P. Olivier, F. Rodriguez-Reinoso, J. Rouquerol and K. S. W. Sing, *Pure Appl. Chem.*, 2015, **87**(9–10), 1051.
30 T. Xue, Y. M. Wang and M.-Y. He, *Microporous Mesoporous Mater.*, 2012, **156**, 29.
31 M. Singh, R. Kamble and N. Viswanadham, *Catal. Lett.*, 2008, **120**, 288.
32 M. M. Mohamed, F. I. Zidan and M. H. Fodail, *J. Mater. Sci.*, 2007, **42**, 4066.
33 J.-H. Kim, M. J. Park, S. J. Kim, O.-S. Joo and K.-D. Jung, *Appl. Catal., A*, 2004, **264**, 37.
34 G. Bonura, M. Cordaro, L. Spadaro, C. Cannilla, F. Arena and F. Frusteri, *Appl. Catal., B*, 2013, **140-141**, 16.
35 D. Mores, J. Kornatowski, U. Olsbye and B. M. Weckhuysen, *Chem. – Eur. J.*, 2011, **17**, 2874.
36 H. G. Karge, *Stud. Surf. Sci. Catal.*, 2001, **137**, 707.
37 P. Castaño, G. Elordi, M. Olazar, A. T. Aguayo, B. Pawelec and J. Bilbao, *Appl. Catal., B*, 2011, **104**, 91.
38 G. Elordi, M. Olazar, G. Lopez, P. Castaño and J. Bilbao, *Appl. Catal., B*, 2011, **102**, 224.

